Next-to-leading order chiral perturbation theory of $K\pi \to \pi$ and $K \to \pi\pi$ amplitudes

Changhoan Kim[1,2]

[1]*Department of Physics, Columbia University, New York, New York 10027, USA*

[2]*School of Physics and Astronomy, University of Southampton, Highfield, Southampton, SO17 1BJ, United Kingdom*

(Received 29 August 2008; revised manuscript received 15 December 2008; published 17 July 2009)

It is shown that the low energy coefficients of the next-to-leading order chiral perturbation theory needed to determine the physical $\Delta I = 1/2$, $K \to \pi\pi$ decay amplitude can be fixed by calculating $K\pi \to \pi$ amplitudes on the lattice. Unlike using next-to-leading order $K \to \pi\pi$ amplitudes proposed by Laiho and Soni, simulating $K\pi \to \pi$ transitions on the lattice does not require evaluations of s-channel disconnected diagrams which have been an obstacle in practice.

DOI: 10.1103/PhysRevD.80.014505 PACS numbers: 12.38.Gc, 12.39.Fe

I. INTRODUCTION

Chiral perturbation theory (χPT) provides a useful tool in understanding the physics of mesons. In particular, it has been employed to extrapolate important quantities to the physical pion mass from the lattice calculations performed using somewhat heavier mesons.

Employing leading order chiral perturbation theory in lattice QCD calculations of nonleptonic kaon decays was proposed by Bernard *et al.* in Refs. [1,2]. In this proposal, the effective weak operators are rewritten in terms of meson fields. The coefficients of those operators (low energy coefficients (LECs)) are determined through lattice simulations where lattice calculations of $K \to$ vac and $K \to \pi$ can be used to determine the more difficult $K \to \pi\pi$ amplitude. This calculation has been done [5,6] with quenched ensembles using the leading order chiral perturbation theory. However, the results did not show a good agreement with the experimental observations.

Since then computing power has drastically improved and we can afford to generate unquenched gauge ensembles. The chiral perturbation theory treatment has also been extended with the next-to-leading order (NLO) calculation done by Laiho and Soni [7]. As mentioned in Ref. [7], the next-to-leading order corrections could be around 30% and the nonzero phase shift of the final $\pi\pi$ state interaction cannot be accommodated by the leading order chiral perturbation theory. Only chiral-loop corrections can induce complex amplitudes.

However, at NLO $K \to \pi\pi_{I=0}$ simulations with unphysically heavy pions in addition to $K \to \pi$ and $K \to$ vac ones on the lattice are needed to determine $K \to \pi\pi$ amplitudes with physical kinematics. There are significant difficulties in lattice calculations of $K \to \pi\pi_{I=0}$ transitions. Those difficulties basically result from the existence of s-channel disconnected diagrams. The numerical evaluation of those diagrams turn out to be very hard because of the exponential decay of signal to noise (SN) ratio. In order to avoid those difficulties, it is proposed to use $K\pi \to \pi$ transitions in Ref. [8].

The most notable advantage of using $K\pi \to \pi$ amplitudes is the elimination of s-channel disconnected diagrams. As one can see from the diagrams shown in Figs. 1 and 4, the $K \to \pi\pi$ and $K\pi \to \pi$ diagrams are related in a one-to-one fashion by simply moving the final π^+ propagator to the initial state. The s-channel disconnected diagram (C) of Fig. 1 is converted to the t-channel disconnected diagram (C) of Fig. 4.

Furthermore, when practical calculations on the lattice are to be performed, a more subtle advantage can be seen. For lattice calculations of $K \to \pi\pi$ amplitudes, in order to ensure that the desired states are projected out, it would be ideal to vary both the separation between the time where the initial state is created and the time where the weak operator is inserted (t_O) and the separation between t_O and the time where the final state is annihilated. However, varying both of the separations may be prohibitly expensive in practice. In this case, it would be most useful to be able to vary the time slice where the two particle state is annihilated (or created for $K\pi \to \pi$ transitions) because the complexity of the two particle state makes it harder to guess *a priori* the appropriate time separation needed to

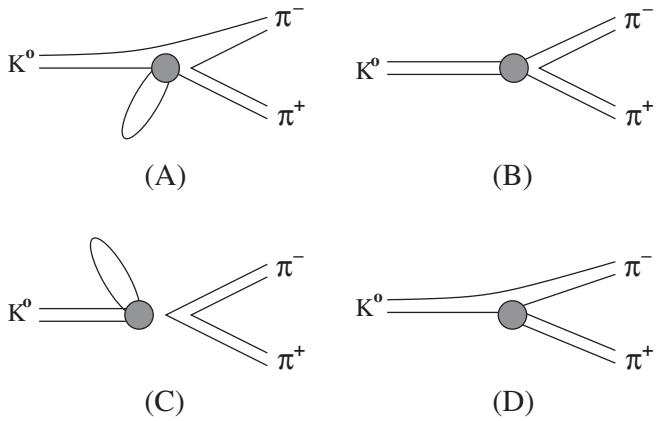

FIG. 1. Quark contraction diagrams for $K \to \pi\pi$ matrix elements. The gray circle represents the insertion of a four-quark operator. By crossing π^+ over the operator, the corresponding diagrams of Fig. 4 are obtained.

project out the desired state. For $K \to \pi\pi$ simulations, the number of fermion propagator inversions must grow proportional to the number of time slices where the $\pi\pi$ state is annihilated, as can be seen from the diagram (C) of Fig. 1. In contrast, for $K\pi \to \pi$ amplitudes, the $K\pi$ state can be created at all time slices with a fixed number of inversions if sources are set at the time where the weak Hamiltonian operator is inserted and also at the time where the π is annihilated.

The same advantage can be exploited when the overlap factors are calculated. Overlap factors, which describe the overlap of the state created by the interpolating operator and the desired state, must be divided out in order to extract transition amplitudes from raw data. In order to compute the overlap factors for the $K \to \pi\pi$ amplitude, simulations of $\pi\pi \to \pi\pi$ ($\pi\pi$ scattering) and $K \to K$ (K spectrum) are required, while for the $K\pi \to \pi$ amplitude, simulations of $K\pi \to K\pi$ ($K\pi$ scattering) and $\pi \to \pi$ (π spectrum) are necessary. Although the $\pi \to \pi$ and $K \to K$ simulations may be equally easy, however, $\pi\pi_{I=0}$ scattering simulations are significantly more difficult than those required for $K\pi$ scattering simulations. As is well known, a calculation of the s-channel disconnected diagrams is required for $\pi\pi_{I=0}$ scattering simulations [8]. In contrast, strangeness conservation ensures that the s-channel disconnected diagrams are not required for $K\pi$ scattering simulations. A more detailed discussion can be found in Ref. [8].

In this paper, the detailed χPT formulae for $K\pi \to \pi$ processes are presented. In the next two sections, we fix notation by expressing the effective weak operators in QCD as elements of the definite irreducible representation of the $SU(3)_L \otimes SU(3)_R$ chiral symmetry group and their corresponding expressions in terms of meson fields follow. Then, it will be explicitly shown that the LECs needed to determine the physical $K \to \pi\pi$ decay amplitude at NLO in χPT can be determined by analyzing the chiral expansion of $K\pi \to \pi$ amplitudes at simple kinematic points. Those effects of finite volume are discussed which could be an issue when two particle states with nonzero relative momentum are considered. Practical issues related to fixing many unknown LECs are also discussed in the later section.

II. EFFECTIVE WEAK OPERATORS

The operator product expansion (OPE) can be used to express $K \to \pi\pi$ decay amplitudes in terms of matrix elements of the $\Delta S = 1$ weak effective Hamiltonian,

$$\langle \pi\pi | \mathcal{H}_{\Delta S=1} | K \rangle = \frac{G_F}{\sqrt{2}} V_{ud} V_{us}^* \sum c_i(\mu) \langle \pi\pi | Q_i(\mu) | K \rangle.$$

In essence, the OPE separates two important physical scales: the $c_i(\mu)$s, called Wilson coefficients, which contain the short distance physics which can be calculated by QCD and electroweak perturbative techniques and the matrix elements $\langle \pi\pi | Q_i(\mu) | K \rangle$, which are determined by the long distance physics for which nonperturbative methods are required. A thorough discussion can be found e.g. in Ref. [9].

If the *charm*-quark is integrated out, there are 10 of $Q_i(\mu)$. Since they have been tabulated many times [10], only two of them are shown, here:

$$Q_1 = \bar{s}_a \gamma_\mu (1 - \gamma^5) u_a \bar{u}_b \gamma^\mu (1 - \gamma^5) d_b, \tag{1}$$

$$Q_7 = \frac{3}{2} \bar{s}_a \gamma_\mu (1 - \gamma^5) d_a \sum_q e_q \bar{q}_b \gamma^\mu (1 + \gamma^5) q_b. \tag{2}$$

The Q_1 is called a current-current weak operator and the O_7 arises from electroweak penguin diagrams.

In order to use chiral perturbation theory, these operators must be written in terms of elements of irreducible representations of the chiral symmetry group. The relevant four-quark operators can be arranged into irreducible representations of the $SU(3)_L \otimes SU(3)_R$ chiral group with definite isospin as follows:

$$\mathcal{X}^{(3/2)}_{\mathbf{27,1}} = (\bar{s}d)_L [(\bar{u}u)_L - (\bar{d}d)_L] + (\bar{s}u)_L (\bar{u}d)_L,$$

$$\mathcal{X}^{(1/2)}_{\mathbf{27,1}} = (\bar{s}d)_L [(\bar{u}u)_L + 2(\bar{d}d)_L - 3(\bar{s}s)_L] + (\bar{s}u)_L (\bar{u}d)_L,$$

$$\mathcal{X}^{(1/2)}_{\mathbf{8,1}} = (\bar{s}d)_L (\bar{u}u)_L - (\bar{s}u)_L (\bar{u}d)_L,$$

$$\tilde{\mathcal{X}}^{(1/2)}_{\mathbf{8,1}} = (\bar{s}d)_L [(\bar{u}u)_L + 2(\bar{d}d)_L + 2(\bar{s}s)_L] + (\bar{s}u)_L (\bar{u}d)_L,$$

$$\mathcal{Y}^{(1/2)}_{\mathbf{8,1}} = (\bar{s}d)_L [(\bar{u}u)_R + (\bar{d}d)_R + (\bar{s}s)_R],$$

$$\mathcal{Y}^{(1/2)c}_{\mathbf{8,1}} = \{(\bar{s}d)_L [(\bar{u}u)_R + (\bar{d}d)_R + (\bar{s}s)_R]\}^c,$$

$$\mathcal{Y}^{(3/2)}_{\mathbf{8,8}} = (\bar{s}d)_L [(\bar{u}u)_R - (\bar{d}d)_R] + (\bar{s}u)_L (\bar{u}d)_R,$$

$$\mathcal{Y}^{(3/2)c}_{\mathbf{8,8}} = \{(\bar{s}d)_L [(\bar{u}u)_R - (\bar{d}d)_R]\}^c + \{(\bar{s}u)_L (\bar{u}d)_R\}^c,$$

$$\mathcal{Y}^{(1/2)}_{\mathbf{8,8}} = (\bar{s}d)_L [(\bar{u}u)_R - (\bar{s}s)_R] - (\bar{s}u)_L (\bar{u}d)_R,$$

$$\mathcal{Y}^{(1/2)c}_{\mathbf{8,8}} = \{(\bar{s}d)_L [(\bar{u}u)_R - (\bar{s}s)_R]\}^c - \{(\bar{s}u)_L (\bar{u}d)_R\}^c,$$

where we follow the notation of Ref. [6]. Operators are classified by the Lorentz structure $L \otimes L$ and $L \otimes R$ and represented by $\mathcal{X}$ and $\mathcal{Y}$, respectively. The irreducible representation to which the operator belongs is given in the subscript and the short hand notation

$$(\bar{s}d)_L = \bar{s}^a \gamma_\mu (1 - \gamma_5) d^a, \qquad (\bar{s}d)_R = \bar{s}^b \gamma_\mu (1 + \gamma_5) d^b$$

is used. Because of invariance under the Fierz transformation, there are no color mixed $L \otimes L$ operators appearing, but for $L \otimes R$ operators, their color mixed versions are represented by superscript c:

$$\{(\bar{s}d)_L(\bar{s}d)_R\}^c = \bar{s}^a\gamma_\mu(1-\gamma_5)d^b\bar{s}^b\gamma_\mu(1+\gamma_5)d^a. \quad (3)$$

Finally, the isospin of the operators is also given in the superscript.

In terms of this basis, the four-quark operators are rewritten as

$$Q_1 = \tfrac{1}{2}\mathcal{X}^{(1/2)}_{\mathbf{8,1}} + \tfrac{1}{10}\tilde{\mathcal{X}}^{(1/2)}_{\mathbf{8,1}} + \tfrac{1}{15}\mathcal{X}^{(1/2)}_{\mathbf{27,1}} + \tfrac{1}{3}\mathcal{X}^{(3/2)}_{\mathbf{27,1}}, \quad (4)$$

$$Q_7 = \tfrac{1}{2}[\mathcal{Y}^{(1/2)}_{\mathbf{8,8}} + \mathcal{Y}^{(3/2)}_{\mathbf{8,8}}]. \quad (5)$$

The strategy is to measure the matrix elements of the $\mathcal{X}$ and $\mathcal{Y}$ operators with quarks somewhat heavier than physical quarks and to use the chiral expansion to extrapolate the matrix elements to the physical quark mass. Then, we can recover the matrix elements of the $Q_i(\mu)$ operators from Eqs. (4) and (5).

Note that the classification of the $\mathcal{X}$ and $\mathcal{Y}$ operators relies on the chiral symmetry. Thus, the realization of the chiral symmetry on the lattice is crucial. Since Ginsparg-Wilson fermions can allow extrapolation to the chiral limit without taking continuum limit, using a lattice formulation of one of those fermions is necessary for the calculations of the matrix elements.

At leading order in the chiral expansion, which will be defined in the next section, the $K\pi \to \pi$ transition amplitude can be written

$$\langle\pi|O^{(8,1)}|K\pi\rangle = \frac{i}{f^3}\Big(\alpha_2(m_K^2 - m_\pi^2)\Big(\frac{8}{3} + \frac{4i(-m_\pi^2 + 2(p_K\cdot p_\pi) + (p_K\cdot k_\pi) + (p_\pi\cdot k_\pi))}{3(m_\pi^2 + (p_K\cdot p_\pi) - (p_K\cdot k_\pi) - (p_\pi\cdot k_\pi))}\Big) - 4\alpha_1((p_K\cdot k_\pi) - (p_\pi\cdot k_\pi))\Big), \quad (6)$$

where α_1 and α_2 are unknown LECs and will be determined by comparing with lattice calculations of e.g.

$$F_V\langle\pi|\mathcal{Y}^{(1/2)}_{\mathbf{8,1}}|K\pi\rangle, \quad (7)$$

where F_V is the Lüscher-Lellouch finite volume factor [11]. One can easily see from Eq. (6) that by varying momentum and mass the unknown coefficients can be determined [12]. We can then use Eq. (6) to reduce the physical $K \to \pi\pi$ transition amplitude by setting $p_K = (m_K, 0)$, $p_\pi = (-m_K/2, \mathbf{k})$, and $k_\pi = (m_K/2, \mathbf{k})$ with $m_K = 2\sqrt{m_\pi^2 + \mathbf{k}^2}$.

Note that there are other operators belonging to the same chiral representation (e.g. $\mathcal{X}^{(1/2)}_{\mathbf{8,1}}$). For those operators, the same analysis can be done with different values of LECs.

III. CHIRAL PERTURBATION THEORY

Chiral perturbation theory (χPT) is based on an effective field theory of the low energy sector of QCD. Its fundamental degrees of freedom are the lowest mass pseudoscalar mesons which are the Goldstone-bosons arising from spontaneous chiral symmetry breaking. Because of the nonlinear transformation of the Goldstone-bosons under the symmetry group, the meson fields appear in the field Σ given by

$$\Sigma = \exp\Big[\frac{2i\phi^a t^a}{f}\Big], \quad (8)$$

where Σ belongs to the $(3, \bar{3})$ representation of the $SU(3)_L \otimes SU(3)_R$, the 3×3 matrices t^a are proportional to the Gell-Mann matrices with $\mathrm{tr}(t_a t_b) = \delta_{ab}$, and the ϕ^a are the real pseudoscalar-meson fields. The quantity f is the meson decay constant in the chiral limit, with f_π equal to 130 MeV in this notation [7].

The leading order ($O(p^2)$) strong Lagrangian is given by

$$\mathcal{L}^{(2)}_{\mathrm{st}} = \frac{f^2}{8}\,\mathrm{tr}[\partial_\mu\Sigma^\dagger\partial^\mu\Sigma] + \frac{f^2 B_0}{4}\,\mathrm{tr}[\chi^\dagger\Sigma + \Sigma^\dagger\chi], \quad (9)$$

where χ is a diagonal mass matrix with its diagonal elements (m_u, m_d, m_s). They are related to the meson mass via

$$B_0 = \frac{m^2_{\pi^+}}{m_u + m_d} = \frac{m^2_{K^+}}{m_u + m_s} = \frac{m^2_{K^0}}{m_d + m_s}. \quad (10)$$

The leading order weak Lagrangian is given by

$$\mathcal{L}^{(2)}_W = \alpha_1\,\mathrm{tr}[\lambda_6\partial_\mu\Sigma^\dagger\partial^\mu\Sigma] + \alpha_2 2B_0\,\mathrm{tr}[\lambda_6(\chi^\dagger\Sigma + \Sigma^\dagger\chi)] + \alpha_{27}t^{ij}_{kl}(\Sigma^\dagger\partial_\mu\Sigma)^k_i(\Sigma^\dagger\partial^\mu\Sigma)^l_j + \alpha_{88}\,\mathrm{tr}[\lambda_6\Sigma^\dagger Q\Sigma] + \mathrm{H.c.}, \quad (11)$$

where terms with coefficients α_1 and α_2 belong to the (8, 1) representation of the $SU(3)_L \otimes SU(3)_R$ group and the last two terms belong to the (27, 1) and the (8, 8) representation, respectively.

The Lagrangian of the next-to-leading order ($O(p^4)$) weak operators may be written

$$\mathcal{L}^{(4)}_W = \sum e_i\mathcal{O}^{(8,1)}_i + \sum d_i\mathcal{O}^{(27,1)}_i + \sum c_i\mathcal{O}^{(8,8)}_i. \quad (12)$$

The complete set of NLO weak operators with $\Delta S = 1$ is discussed by Kambor, Missimer, and Wyler in Ref. [13]. A minimal subset of operators contributing $K \to \pi$ and $K \to \pi\pi$ processes are studied in Refs. [14–17] and the explicit forms are given in Refs. [7,17,18].

The (8, 8) and (27, 1) operators will not be considered in this paper since the LECs for those operators can be determined without $\Delta I = 1/2$, $K \to \pi\pi$ simulations [19]. The explicit forms of the (8, 1) operators are

$$\mathcal{O}_1^{(8,1)} = \mathrm{tr}[\lambda_6 S^2], \qquad \mathcal{O}_2^{(8,1)} = \mathrm{tr}[\lambda_6 S]\mathrm{tr}[S],$$
$$\mathcal{O}_3^{(8,1)} = \mathrm{tr}[\lambda_6 P^2], \qquad \mathcal{O}_4^{(8,1)} = \mathrm{tr}[\lambda_6 P]\mathrm{tr}[P],$$
$$\mathcal{O}_5^{(8,1)} = \mathrm{tr}[\lambda_6 [S, P]], \qquad \mathcal{O}_{10}^{(8,1)} = \mathrm{tr}[\lambda_6 \{S, L^2\}],$$
$$\mathcal{O}_{11}^{(8,1)} = \mathrm{tr}[\lambda_6 L_\mu S L^\mu], \qquad \mathcal{O}_{12}^{(8,1)} = \mathrm{tr}[\lambda_6 L_\mu]\mathrm{tr}[\{L^\mu, S\}],$$
$$\mathcal{O}_{13}^{(8,1)} = \mathrm{tr}[\lambda_6 S]\mathrm{tr}[L^2], \qquad \mathcal{O}_{15}^{(8,1)} = \mathrm{tr}[\lambda_6 [P, L^2]],$$
$$\mathcal{O}_{35}^{(8,1)} = \mathrm{tr}[\lambda_6 \{L_\mu, \partial_\nu W^{\mu\nu}\}], \qquad \mathcal{O}_{39}^{(8,1)} = \mathrm{tr}[\lambda_6 W_{\mu\nu} W^{\mu\nu}]$$

with $S = 2B_0(\chi^\dagger \Sigma + \Sigma^\dagger \chi)$, $P = 2B_0(\chi^\dagger \Sigma - \Sigma^\dagger \chi)$, $L_\mu = i\Sigma^\dagger \partial_\mu \Sigma$, $W^{\mu\nu} = 2(\partial_\mu L_\nu + \partial_\nu L_\mu)$, and $(\lambda_6)_{ij} = \delta_{3i}\delta_{2j}$.

Finally, the next-to-leading order strong Lagrangian relevant for kaon decay amplitudes is

$$\mathcal{L}_{\mathrm{st}}^{(4)} = \sum L_i \mathcal{O}_i^{(\mathrm{st})} \tag{13}$$

and the explicit forms for the $\mathcal{O}_i^{(\mathrm{st})}$ are

$$\mathcal{O}_1^{(\mathrm{st})} = \mathrm{tr}[L^2]^2, \qquad \mathcal{O}_2^{(\mathrm{st})} = \mathrm{tr}[L_\mu L_\nu]\mathrm{tr}[L^\mu L^\nu],$$
$$\mathcal{O}_3^{(\mathrm{st})} = \mathrm{tr}[L^2 L^2], \qquad \mathcal{O}_4^{(\mathrm{st})} = \mathrm{tr}[L^2]\mathrm{tr}[S],$$
$$\mathcal{O}_5^{(\mathrm{st})} = \mathrm{tr}[L^2 S], \qquad \mathcal{O}_6^{(\mathrm{st})} = \mathrm{tr}[S]^2,$$
$$\mathcal{O}_8^{(\mathrm{st})} = \tfrac{1}{2}\mathrm{tr}[S^2 + P^2]. \tag{14}$$

IV. ROLE OF $K\pi \to \pi$ MATRIX ELEMENTS

In this section, we will show explicitly that those LECs necessary to calculate the physical $K \to \pi\pi$ amplitude can be determined from $K \to$ vac, $K \to \pi$, and $K\pi \to \pi$ amplitudes.

There are five types of operators depending on the representation of the chiral group and isospin: (27, 1) $\Delta I = 3/2$, (27, 1) $\Delta I = 1/2$,(8, 8) $\Delta I = 1/2$,(8, 8) $\Delta I = 3/2$, and (8, 1) $\Delta I = 1/2$. In this paper, only (8, 1) $\Delta I = 1/2$ operators are discussed. LECs for other operators (27, 1)/(8, 8) $\Delta I = 1/2$ or $3/2$ can be determined without the use of $K \to \pi\pi_{I=0}$ amplitudes [19].

In order to check that all the LECs sufficient to reconstruct the physical $K \to \pi\pi$ amplitude can be determined, it is enough to look at the analytic terms. Since matrix elements, meson masses, and the meson momenta are calculated on the lattice, if we insert those quantities into the following χPT formulae a set of linear equations of LECs will be obtained. Presumably, the contribution of the logarithm terms would not render the linear equations singular. So, we omit the logarithmic terms in the following formulae.

Although $K \to$ vac and $K \to \pi$ calculations have already been done, for example, in Ref. [7], we present the formulae for completeness. The analytic terms in the $K \to$ vac amplitude come from diagrams T1 and T2 of Fig. 2 and they are

$$\langle 0|\mathcal{O}^{(8,1)}|K^0\rangle = -\frac{4i\alpha_2(m_K^2 - m_\pi^2)}{f} - \frac{8i(m_K^2 - m_\pi^2)(2(e_1 + e_2 + e_5)m_K^2 + e_2 m_\pi^2)}{f}. \tag{15}$$

From this calculation, one can determine α_2, e_2, $e_1 + e_5$. If *CPS* [21] symmetry [22] is realized, hence $m_K = m_\pi$, the $K \to$ vac matrix elements vanish. Thus, nondegenerate quark masses must be used for the determination of these LECs.

The diagrams E1 and E2 of Fig. 3 generate the analytic terms in the $K \to \pi$ amplitudes, which are

$$\langle \pi^+(k_\pi)|\mathcal{O}^{(8,1)}|K^+(p_K)\rangle = \frac{4\alpha_1(p_K \cdot k_\pi) - 4\alpha_2 m_K^2}{f^2} + \frac{1}{f^2}(-16(e_1 + e_2 + e_5)m_K^4 + (16(e_{10} - e_{35})(p_K \cdot k_\pi) - 8(e_2 + 2e_3 - 2e_5)m_\pi^2)m_K^2 + 64e_{39}(p_K \cdot k_\pi)^2 + 8(e_{11} - 2e_{35})(p_K \cdot k_\pi)m_\pi^2). \tag{16}$$

By varying momenta and masses, one can determine α_1, e_{39}, $e_{11} - 2e_{35}$, $e_{10} - e_{35}$, and $e_3 - e_5$ when combined with $K \to$ vac results.

For $K\pi \to \pi$, there are five diagrams: A1, A2, and C1 of Fig. 2 and G1 and G2 of Fig. 3. The analytic terms are

$$\begin{aligned}\langle \pi^-(k_\pi)|\mathcal{O}^{(8,1)}|K^0(p_K)\pi^-(p_\pi)\rangle_{G1+G2} = \frac{i}{f^3}\Big(&\frac{8}{3}\alpha_2(m_K^2 - m_\pi^2) - 4\alpha_1((p_K \cdot k_\pi) - (p_\pi \cdot k_\pi)) + \frac{32}{3}(e_1 + e_2 + e_5)m_K^4 \\ &+ \frac{16}{3}(e_1 + 5e_2 + 3e_3 - 2e_5)m_\pi^2 m_K^2 - 16((e_{10} - e_{35})(p_K \cdot k_\pi) \\ &+ (2e_{13} + e_{15})(p_\pi \cdot k_\pi))m_K^2 - \frac{16}{3}(3e_1 + 7e_2 + 3e_3)m_\pi^4 - 64e_{39}((p_K \cdot k_\pi)^2 \\ &- (p_\pi \cdot k_\pi)^2) - 8(e_{11} - 2(e_{15} + e_{35}))(p_K \cdot k_\pi)m_\pi^2 \\ &+ 8(2e_{10} + e_{11} + 4e_{13} - 4e_{35})(p_\pi \cdot k_\pi)m_\pi^2 \\ &+ 16e_{35}(p_K \cdot p_\pi)((p_K \cdot k_\pi) - (p_\pi \cdot k_\pi))\Big),\end{aligned} \tag{17}$$

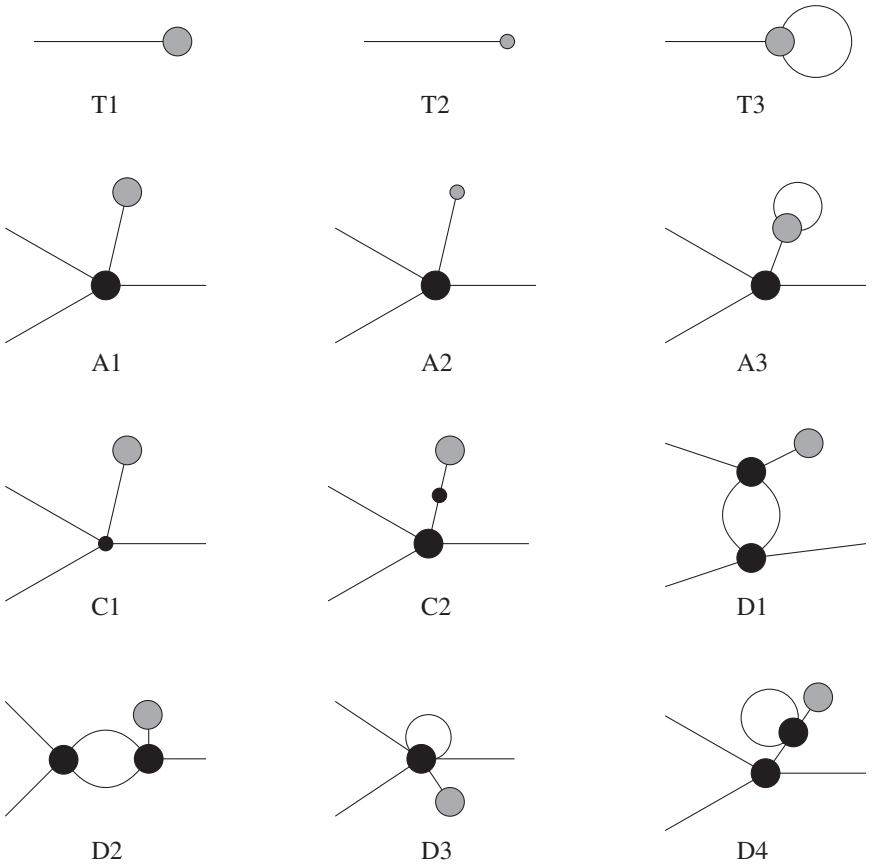

FIG. 2. Diagrams involved with tadpoles. T1, T2, and T3 are relevant to $K \to$ vac amplitudes while others are for $K\pi \to \pi$ amplitudes. Gray (black) blobs are weak (strong) vertices. Large blobs are the leading order terms while the small blobs are the next-to-leading order ones.

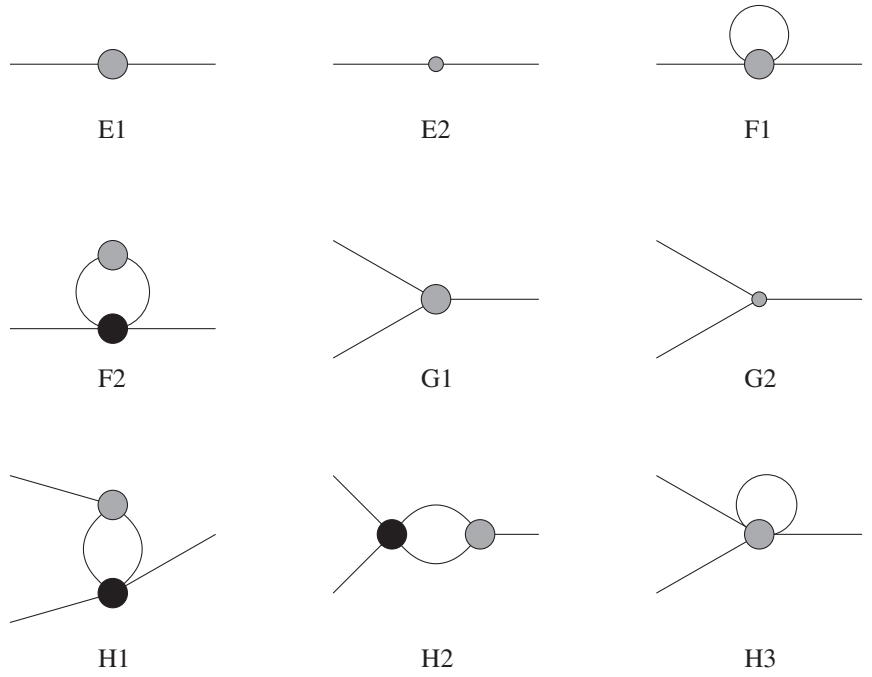

FIG. 3. Diagrams not involved with tadpoles. E1, E2, and F1 are relevant to $K \to \pi$ amplitudes while others are for $K\pi \to \pi$ amplitudes. Gray (black) blobs are weak (strong) vertices. Large blobs are the leading order terms while the small blobs are the next-to-leading order ones.

$$\langle\pi^-(k_\pi)|\mathcal{O}^{(8,1)}|K^0(p_K)\pi^-(p_\pi)\rangle_{A1+A2} = \frac{4i(-m_\pi^2+2(p_K\cdot p_\pi)+(p_K\cdot k_\pi)+(p_\pi\cdot k_\pi))(m_\pi^2-m_K^2)(\alpha_2+4(e_1+e_2+e_5)m_K^2+2e_2m_\pi^2)}{3f^3(m_\pi^2+(p_K\cdot p_\pi)-(p_K\cdot k_\pi)-(p_\pi\cdot k_\pi))}, \tag{18}$$

and

$$\begin{aligned}\langle\pi^-(k_\pi)|\mathcal{O}^{(8,1)}|K^0(p_K)\pi^-(p_\pi)\rangle_{C1} = {}& \frac{i16\alpha_2(m_K^2-m_\pi^2)}{3f^5(p_k+p_\pi-k_\pi)^2-m_K^2}(-12k_\pi\cdot p_Kk_\pi\cdot p_\pi(2L_1+L_2+L_3)\\ &+6p_K\cdot p_\pi(k_\pi\cdot p_\pi(4L_1+2L_2+L_3)+k_\pi\cdot p_K(4L_2+L_3))\\ &+2k_\pi\cdot p_\pi(12L_1+3L_3-8L_4-L_5)m_K^2-4p_K\cdot p_\pi(2L_4+L_5)m_K^2-(2L_4+L_5\\ &-2(2L_6+L_8))m_K^4-2k_\pi\cdot p_K(2L_4+L_5)m_K^2+2k_\pi\cdot p_K(6L_2+3L_3+5L_4)m_\pi^2\\ &-2k_\pi\cdot p_\pi L_4m_\pi^2-(11L_4+4L_5-6(5L_6+2L_8))m_K^2m_\pi^2\\ &-2p_K\cdot p_\pi(6L_2+8L_4+3L_5)m_\pi^2+(L_4-L_5+2(L_6+L_8))m_\pi^4),\end{aligned} \tag{19}$$

where the L_i are Gasser-Leutwyler coefficients [23], and it is assumed that those coefficients are already known [24].

Since the analytic terms of $K\pi\to\pi$ amplitudes are quite complex, we isolate the new coefficients which must be determined from $K\pi\to\pi$ amplitudes by inserting LECs that can be computed from $K\to$ vac and $K\to\pi$ amplitudes. One can easily see that only three coefficients remain to be determined which are from the G2 contribution,

$$\begin{aligned}\langle\pi^-(k_\pi)|\mathcal{O}^{(8,1)}|K^0(p_K)\pi^-(p_\pi)\rangle_{G2,\text{part}} = {}& \frac{i}{f^3}(16e_{35}(p_K\cdot p_\pi)((p_K\cdot k_\pi)-(p_\pi\cdot k_\pi))-32e_{13}(p_\pi\cdot k_\pi)(m_K^2-m_\pi^2)\\ &-16e_{15}((p_\pi\cdot k_\pi)m_K^2-(p_K\cdot k_\pi)m_\pi^2)).\end{aligned} \tag{20}$$

In order to show explicitly that the needed coefficients can be determined, we choose kinematics where the initial kaon and pion are nearly at rest while the final pion has momentum $2\pi/L$. With these kinematic points,

$$\langle\pi^-(k_\pi)|\mathcal{O}^{(8,1)}|K^0(p_K)\pi^-(p_\pi)\rangle_{G2,\text{part}} = \frac{16iW((e_{35}-e_{15})(W_\pi m_K^2-W_Km_\pi^2)-e_{13}(E_W+W_\pi)(m_K^2-m_\pi^2))}{f^3}, \tag{21}$$

where W is the energy of the final pion and W_K and W_π are the energies of the initial kaon and pion, respectively. Although very small, we take into account the momentum of the initial particles. When $K\pi\to\pi$ transitions are simulated on the lattice, this small momentum originates from interactions between the kaon and the pion and we have no control over the direction of this momentum. An average over solid angle must be taken. More discussion of this point is given in Sec. V. This effect is already included in the above formula. Now, one can see that $e_{35}-e_{15}$ and e_{13} can be determined by varying m_K and m_π. Then, combined with $K\to$ vac and $K\to\pi$ results, one can determine the NLO analytic terms of the physical $K\to\pi\pi$ matrix element:

$$\begin{aligned}&\langle\pi^-\pi^+|\mathcal{O}^{(8,1)}|K^0\rangle_{\text{PHYS}}\\ &=\frac{8i}{f^3}(m_K^2-m_\pi^2)\cdot(((e_{10}-e_{35})+(e_{35}-e_{15})-2e_{13})m_K^2\\ &\quad+(-2(e_1+e_5)-4e_2-2(e_3-e_5)+2(e_{10}-e_{35})\\ &\quad+(e_{11}-2e_{35})+4e_{13}+8e_{39})m_\pi^2).\end{aligned}$$

Note that the SU(3) limit cannot be used because Eq. (21) vanishes in that limit. Moreover, there is a further restriction on the choice of momenta if one considers more general kinematics. The tadpole contribution (Eqs. (18) and (19)) can diverge for some choices of momenta [26]. This is a disadvantage of using transitions with an unavoid-

able energy-momentum injection such as the current proposal.

V. FINITE VOLUME EFFECTS

In the previous section, it is shown that the unknown LECs can be determined by measuring weak matrix elements from lattice calculations. We choose to use a minimal set of matrix elements for the sake of proving sufficiency of the calculation of only these types of amplitudes. However, as is suggested in the next section, it would be useful to measure more matrix elements rather than the minimal set so that one can reduce statistical errors in determining the LECs and test for the consistency of the χPT expansions.

An obvious approach is to include matrix elements with mesons of different masses, but this requires new sets of configuration if we want to use unquenched chiral perturbation theory. A method which does not require new ensembles is to use mesons with nonzero relative momenta. In this case, the nontrivial finite volume effects on the resulting matrix elements are not exponentially small. This has been studied by Lüscher and Lellouch in Ref. [11] and it is generalized to the case where the total momentum is not zero in Refs. [28,29]. This generalization is quite useful since using a system with nonzero total momentum is the only method, at the moment, of creating two particle states with nonzero relative momentum without generating new gauge ensembles.

One can also consider matrix elements that spatial momentum is injected through the weak Hamiltonian. In such cases, the result of Refs. [28,29] has to be generalized further. This is straightforward and the derivation is given in Appendix B. The final result is

$$|\langle\pi(\mathbf{k})|H_W(0)|K\pi,(E,\mathbf{P})\rangle| = \frac{1}{4\pi}\frac{1}{\sqrt{\rho_V}}\sqrt{\frac{\pi}{(2\pi)^3}\left(\frac{q^*}{E^*}\right)} \times \left|\int d\Omega_{E^*}\langle\pi(\mathbf{k}^*)|H_W(0)|K(\mathbf{q})\pi(-\mathbf{q})\rangle\right|, \quad (22)$$

where the left-hand side represents a matrix element in a finite box while the integrand on the right-hand side represents one in an infinite volume. Here, E is the energy of the $K\pi$ state which can be measured from lattice calculations. Similarly, $\mathbf{P}$ is the total momentum of the $K\pi$ state which is imposed explicitly by the operator creating the state. Finally, $\mathbf{k}$ is the momentum of the final pion. The starred variables are those Lorentz-transformed into the center of momentum (CM) frame. In particular,

$$E^* \equiv \sqrt{E^2 - P^2} \quad (23)$$

which in turn gives the Lorentz transformation angle $\beta = P/E$ and the q^* is defined from

$$E^* = \sqrt{m_K^2 + q^{*2}} + \sqrt{m_\pi^2 + q^{*2}}. \quad (24)$$

The $\mathbf{k}^*$ is the result of the Lorentz transformation with the above β of the four-momentum of the final pion state, $(\sqrt{m_\pi^2 + \mathbf{k}^2}, \mathbf{k})$. ρ_V is a function of q^* and its definition is given in Refs. [28,29]. Roughly, it can be interpreted as the density of states.

In Eq. (22), the difference from the result of Refs. [28,29] is the explicit appearance of the integration over solid angle. Since the final meson state has nonzero momentum and cannot be used to constrain the initial state to be an S-wave, this must be done explicitly. As such, the initial state in the matrix element $\langle\pi(\mathbf{k})|H_W(0)|K\pi,(E,\mathbf{P})\rangle$ must be in an S-wave state [30], as seen from the CM frame. This means that the S-wave state must be explicitly generated in the lattice simulation. Fortunately, S-wave states are the lowest energy states which can appear, so we can generate the S-wave $K\pi$ state by using any operator which has an overlap with it and evaluating its correlation function for large Euclidean time separation.

VI. PRACTICAL ISSUES

Up until now, the focus of this paper has been that the lattice calculation of $K \to \pi\pi$ matrix elements suggested in Ref. [7] can be replaced with $K\pi \to \pi$ matrix elements which can be measured much more easily than $K \to \pi\pi$ ones. In this section, we address some practical issues associated with the lattice calculation of the matrix elements which are required for determining the LECs.

The strategy this paper has taken is very similar to that of Ref. [7]. Most of the unknown LECs must be determined from $K \to$ vac and $K \to \pi$ matrix elements and $K\pi \to \pi$ matrix elements are considered as supplementary to determine the LECs which cannot be obtained from $K \to$ vac and $K \to \pi$ matrix elements. Since these are simple matrix elements, it is believed that they can be calculated easily with good precision and this has been assumed in the discussion above. Recently, the RBC-UKQCD collaboration has performed a partially quenched calculation of $K \to$ vac and $K \to \pi$ transition amplitudes [31]. As expected, the matrix elements were determined very well. In particular, $K \to \pi$ matrix elements—even after subtraction of the contribution from the mixing with lower dimensional operators—are measured quite accurately with less than 10% error. By employing partial quenching and the corresponding χPT, they attempted to determine from subtracted $K \to \pi$ matrix elements alone, all of the LECs associated $\mathcal{O}^{(8,1)}$ operators except one of the LECs for whose determination another process is required.

Unfortunately, the LECs are determined very poorly, with around 50% to 100% errors.

This escalation of error can be understood easily. The conventional presumption is that LECs follow a multivariate Gaussian distribution with the mean values given by the χPT formulae which can be written, if masses and momenta are known as

$$K(m_K, m_\pi, p_K, p_\pi) \cdot X = \tilde{M}, \tag{25}$$

where we put tildes on M in order to stress that they are theoretical matrix elements. Then, the fitting procedure requires minimizing

$$C(X) = (K \cdot X - M)^T \Sigma^{-1} (K \cdot X - M), \tag{26}$$

where M is the matrix elements measured on the lattice and X represents a vector of the unknown LECs. If the number of unknowns is the same as that of measured matrix elements, the minimization of $C(X)$ is equivalent to solving

$$K(m_K, m_\pi, p_K, p_\pi) \cdot X = M. \tag{27}$$

The point is that even though the errors in M are small there is no guarantee that so are the errors in $K^{-1}M$. For example, if two positive quantities (a, b) with relative errors (e_a, e_b) are subtracted, the relative error of the subtracted value could be significantly larger than e_a or e_b. Indeed, Eqs. (16) and (17) suggest that the difference of the matrix elements must be used to deduce the LECs. In other words, errors in differences of the matrix elements may have more direct impact on the errors of the LECs rather than those of the measured matrix elements do.

If there are redundant matrix elements, the corresponding equation becomes

$$(TK)X = TM \rightarrow (TK)^{-1} TM = X, \tag{28}$$

where matrices K and T are rectangular, not square. The matrix T is determined from the minimization condition of Eq. (26),

$$T = K^T \Sigma^{-1}. \tag{29}$$

The variances of the LECs (i.e. fit parameters) can be written

$$\begin{aligned} \langle X_i X_j \rangle &= \langle [(TK)^{-1} T]_{ik} M_k [(TK)^{-1} T]_{jl} M_l \rangle \\ &= \langle [(K^T \Sigma^{-1} K)^{-1} K^T \Sigma^{-1}]_{ik} \\ &\quad \times M_k [(K^T \Sigma^{-1} K)^{-1} K^T \Sigma^{-1}]_{jl} M_l \rangle. \end{aligned}$$

Utilizing the fact that Σ is the correlation matrix of measured matrix elements, they are simplified into

$$\langle X_i X_j \rangle = [(K^T \Sigma^{-1} K)^{-1}]_{ij}. \tag{30}$$

Note that calculating any linear combination of Ms has no effect on the uncertainties. Such a transformation can be represented by

$$K \rightarrow SK, \qquad \Sigma \rightarrow S \Sigma S^T, \tag{31}$$

and one can see that Eq. (30) is invariant.

Based on Eq. (30), one can consider some schemes to reduce uncertainties of the LECs. An intuitively obvious way, besides increasing the number of configurations, is to increase the number of kinematic points. Although it is evident that more information determines the unknowns more precisely, it is not mathematically apparent from Eq. (30). So, we provide the proof in Appendix D.

In order to enlarge the number of matrix elements, partial quenching may be employed [32]. As mentioned in the earlier section, one can consider imposing various momenta on the pions and kaons. In particular, $K\pi \rightarrow \pi$ transitions can provide a great deal more matrix elements. One of the advantages of $K\pi \rightarrow \pi$ transitions over $K \rightarrow \pi\pi$ ones is that $K\pi \rightarrow \pi$ processes may be simulated with a partially quenched choice of masses. Unlike $K \rightarrow \pi\pi$ transitions which require unitarity, $K\pi \rightarrow \pi$ matrix elements do not show any pathological behavior on partially quenched ensembles [8]. Thus, those additional inversions required for partially quenched $K \rightarrow \pi$ matrix element calculations can be used for $K\pi \rightarrow \pi$ matrix elements.

There is no data discussing fluctuations of lattice correlation functions for $K\pi \rightarrow \pi$ matrix elements. In Fig. 4, the quark contraction diagrams for $K\pi \rightarrow \pi$ transitions are shown. Since the diagrams (B) and (D) are essentially the same as those appearing $K \rightarrow \pi\pi_{I=2}$ transitions, we know that the signal to noise ratios are as good as those of lattice correlation functions of $K \rightarrow \pi\pi_{I=2}$ transitions. The SN ratios of (A) and (C) are hard to estimate, but one may naively imagine that the effect of the loop in the middle is as mild as the case of $K \rightarrow \pi$ matrix elements. Thus, one might expect the errors of lattice calculations of $K\pi \rightarrow \pi$ matrix elements are as small as those of $K \rightarrow \pi$ matrix elements.

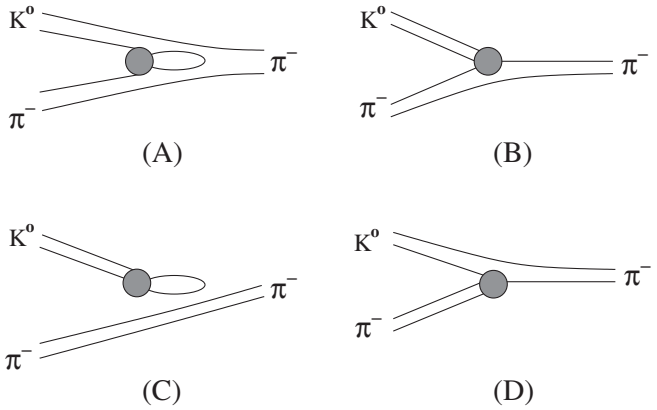

FIG. 4. Quark contraction diagrams for $K\pi \to \pi$ transitions. The gray circle represents the insertion of a four-quark operator.

Having many matrix elements, one needs a large number of configurations in order to estimate the correlation matrix reliably. It has been argued that the number of configurations must be around 10 times that of observables [33]. Since a large number of configurations are needed to reduce to statistical errors in matrix elements, increasing the number of configurations is imperative. Indeed, the number of configurations used by the RBC-UKQCD collaboration was around 70. If the number of configurations may be quadrupled, hence around 300, the errors on matrix elements will go down by a factor of 2 and we can have 30 matrix elements which is almost three times as many as the numbers of the unknown LECs, which could make additional improvement of accuracy of the determination of the LECs. It is notable that the covariance matrix (Eq. (30)) may become smaller even though matrix elements inconsistent with the fit function are included. Thus, the χ^2 of the fit must be monitored when more information is exploited.

Determining all the LECs necessary to extrapolate the real world $K \to \pi\pi$ matrix elements is certainly a numerically challenging task. Nevertheless, it is so only because of the unusually large number of parameters to fit. As discussed earlier, measuring more matrix elements than the number of unknowns is essential besides increasing statistics. This could be achieved by employing partial quenching and by including $K\pi \to \pi$ processes as well as $K \to$ vac and $K \to \pi$ ones.

VII. SUMMARY

In this paper, it is shown that the LECs necessary for the NLO χPT extrapolation of the physical $\langle\pi\pi|\mathcal{O}^{(8,1)}|K\rangle$ matrix elements can be obtained from lattice calculations of $K\pi \to \pi$, $K \to \pi$, and $K \to$ vac processes. The important point is that simulations of $K \to \pi\pi_{I=0}$ transitions, which are very difficult, can be avoided.

Although we establish this result by using a minimal set of kinematics, in practice one may want to use as many matrix elements as the ensemble size allows. In order to enlarge the number of matrix elements, one can consider including more kinematics as well as employing partial quenching. Unlike $K \to \pi\pi$ processes, $K\pi \to \pi$ ones can be simulated on partially quenched ensembles. If nontrivial kinematic points are to be used, the finite volume effects on $K\pi \to \pi$ matrix elements must be taken into account carefully [11]. In particular, the case where spatial momentum is injected through the weak Hamiltonian is discussed, which requires a slight generalization of the results of Ref. [28].

As discussed in Ref. [8], using $K\pi \to \pi$ processes allows us to avoid technical difficulties such as s-channel disconnected diagrams. However, the mixing with lower dimensional operators is still present. One may apply the subtraction scheme used in Ref. [5].

The current computing resources are powerful enough to simulate $K\pi \to \pi$ transitions. With these NLO χPT formulae, we can improve the calculation of $K \to \pi\pi$ matrix elements, which in turn will allow us to evaluate ϵ'/ϵ more accurately.

However, the recent work by the RBC-UKQCD collaboration showed some concern regarding the validity of SU(3) χPT as their data did not fit very well [25,31]. If this turns out to be generally true, the approach of using χPT for extrapolating $K \to \pi\pi$ matrix elements to the physical point may need to be reconsidered [34].

ACKNOWLEDGMENTS

The author thanks Christopher Sachrajda, Norman Christ, and Chris Dawson for useful discussions and Michael Endres and Matthew Lightman for reading the manuscript. The author acknowledges that some of the calculations in this paper are done by FEYNARTS package [37] on MATHEMATICA. This research is supported by PPARC Grants No. PPA/G/O/2002/00468 and No. PPA/G/S/2003/00093, by DOE Grant No. DE-FG02-96ER40956, and by the RIKEN-BNL Research Center.

APPENDIX A: LOGARITHMIC TERMS

In this section, the logarithmic terms (diagram A3, F1, F2, D1, D2, D3, H1, H2, H3) are given.

1. The integrals

In order to write the transition amplitude in a simpler form, the following notations are used:

$$A_0(m) \equiv \mu^\epsilon \int \frac{d^d q}{(2\pi)^d} \frac{1}{q^2 - m^2},$$

$$A_1(m) \equiv \mu^\epsilon \int \frac{d^d q}{(2\pi)^d} \frac{q^2}{q^2 - m^2},$$

$$B_0(m_1,m_2,k) \equiv \mu^\epsilon \int \frac{d^dq}{(2\pi)^d} \frac{1}{(q-k)^2-m_1^2} \frac{1}{(q+k)^2-m_2^2},$$
$$B_{0\mu}(m_1,m_2,k) \equiv \mu^\epsilon \int \frac{d^dq}{(2\pi)^d} \frac{q_\mu}{(q-k)^2-m_1^2} \frac{1}{(q+k)^2-m_2^2},$$
$$B_{0\mu\nu}(m_1,m_2,k) \equiv \mu^\epsilon \int \frac{d^dq}{(2\pi)^d} \frac{q_\mu}{(q-k)^2-m_1^2} \frac{q_\nu}{(q+k)^2-m_2^2},$$
$$B_1(m_1,m_2,k) \equiv \mu^\epsilon \int \frac{d^dq}{(2\pi)^d} \frac{q^2}{(q-k)^2-m_1^2} \frac{1}{(q+k)^2-m_2^2},$$
$$B_{1\mu}(m_1,m_2,k) \equiv \mu^\epsilon \int \frac{d^dq}{(2\pi)^d} \frac{q_\mu}{(q-k)^2-m_1^2} \frac{q^2}{(q+k)^2-m_2^2},$$
$$B_2(m_1,m_2,k) \equiv \mu^\epsilon \int \frac{d^dq}{(2\pi)^d} \frac{q^2}{(q-k)^2-m_1^2} \frac{q^2}{(q+k)^2-m_2^2}.$$

Furthermore, when there is a Lorentz contraction, we use the following abbreviation:

$$k \cdot B_0 \equiv B_{0\mu} k^\mu, \qquad k \cdot B_1 \equiv B_{1\mu} k^\mu, \qquad p \cdot B_0 \cdot k \equiv p^\mu B_{0\mu\nu} k^\nu.$$

2. Diagram H1a

Here, $q = \frac{1}{2}(p_\pi - k_\pi)$,

$$\begin{aligned}
\langle \pi^-(k_\pi)|\mathcal{O}^{(8,1)}|K^0(p_K)\pi^-(p_\pi)\rangle_{H1a} = \frac{1}{f^5\pi^2}\Big(&4\alpha_1 k_\pi \cdot B_0(q,m_K,m_K)\cdot p_K + 8\alpha_1 k_\pi \cdot B_0(q,m_\pi,m_\pi)\cdot p_K \\
&+ 4\alpha_1 p_\pi \cdot B_0(q,m_K,m_K)\cdot p_K + 8\alpha_1 p_\pi \cdot B_0(q,m_\pi,m_\pi)\cdot p_K \\
&- \frac{2}{3}\alpha_2(4m_K^2-4m_\pi^2)B_1(q,m_K,m_K) + \frac{1}{3}\alpha_1(-2m_K^2-5m_\pi^2+5k_\pi\cdot p_\pi) \\
&\times(-m_\pi^2 - k_\pi\cdot p_K + k_\pi\cdot p_\pi + p_K\cdot p_\pi)B_0(q,m_K,m_K) \\
&+ \frac{1}{3}\alpha_2(-2m_K^2-5m_\pi^2+5k_\pi\cdot p_\pi)(4m_\pi^2-4m_K^2)B_0(q,m_K,m_K) \\
&+ \frac{1}{9}\alpha_2(8m_K^2-8m_\pi^2)(11m_\pi^2-10k_\pi\cdot p_\pi)B_0(q,m_\pi,m_\pi) \\
&+ \frac{1}{9}\alpha_1(-6m_\pi^2-6k_\pi\cdot p_K+6k_\pi\cdot p_\pi+6p_K\cdot p_\pi)(11m_\pi^2-10k_\pi\cdot p_\pi) \\
&\times B_0(q,m_\pi,m_\pi) + \frac{2}{9}\alpha_2(4m_K^2-4m_\pi^2)B_0(q,m_\eta,m_\eta)m_\pi^2 \\
&+ \frac{4}{9}\alpha_2(8m_\pi^2-8m_K^2)B_1(q,m_\pi,m_\pi) + \frac{2}{9}\alpha_1 m_\pi^2(3m_\pi^2+3k_\pi\cdot p_K-3k_\pi\cdot p_\pi \\
&- 3p_K\cdot p_\pi)B_0(q,m_\eta,m_\eta) - \frac{2}{3}\alpha_1(2m_K^2+6m_\pi^2+k_\pi\cdot p_K-6k_\pi\cdot p_\pi-p_K\cdot p_\pi) \\
&\times B_1(q,m_K,m_K) + \frac{4}{9}\alpha_1(39m_\pi^2+6k_\pi\cdot p_K-36k_\pi\cdot p_\pi-6p_K\cdot p_\pi)B_1(q,m_\pi,m_\pi) \\
&- \frac{4}{3}\alpha_1 B_1(q,m_\eta,m_\eta)m_\pi^2 + \frac{4}{3}\alpha_1 B_2(q,m_K,m_K) - \frac{16}{3}\alpha_1 B_2(q,m_\pi,m_\pi)\Big).
\end{aligned}$$

3. Diagram H1b

Here, $q = \frac{1}{2}(p_K - k_\pi)$,

$$\begin{aligned}
\langle \pi^-(k_\pi)|\mathcal{O}^{(8,1)}|K^0(p_K)\pi^-(p_\pi)\rangle_{H1b} = \frac{1}{f^5\pi^2}\Big(&-3\alpha_1 k_\pi\cdot p_K k_\pi\cdot p_\pi B_0(q,m_K,m_\pi) + 3\alpha_1 k_\pi\cdot p_\pi k_\pi\cdot p_\pi B_0(q,m_K,m_\pi)\\
&- \alpha_1 k_\pi\cdot p_K k_\pi\cdot p_\pi B_0(q,m_\eta,m_K) + \alpha_1 k_\pi\cdot p_\pi k_\pi\cdot p_\pi B_0(q,m_\eta,m_K)\\
&- 6\alpha_1 k_\pi\cdot p_\pi B_1(q,m_K,m_\pi) - 2\alpha_1 k_\pi\cdot p_\pi B_1(q,m_\eta,m_K) - 3\alpha_1 k_\pi\cdot p_\pi B_0(q,m_K,m_\pi) p_K\cdot p_\pi\\
&- \alpha_1 k_\pi\cdot p_\pi B_0(q,m_\eta,m_K) p_K\cdot p_\pi - 3\alpha_1 k_\pi\cdot p_K p_K\cdot p_\pi B_0(q,m_K,m_\pi)\\
&+ 3\alpha_1 k_\pi\cdot p_\pi p_K\cdot p_\pi B_0(q,m_K,m_\pi) - 3\alpha_1 p_K\cdot p_\pi p_K\cdot p_\pi B_0(q,m_K,m_\pi) - \alpha_1 k_\pi\\
&\cdot p_K p_K\cdot p_\pi B_0(q,m_\eta,m_K) + \alpha_1 k_\pi\cdot p_\pi p_K\cdot p_\pi B_0(q,m_\eta,m_K) - \alpha_1 p_K\cdot p_\pi p_K\\
&\cdot p_\pi B_0(q,m_\eta,m_K) - 6\alpha_1 p_K\cdot p_\pi B_1(q,m_K,m_\pi) - 2\alpha_1 p_K\cdot p_\pi B_1(q,m_\eta,m_K) - \frac{5}{3}\alpha_1 k_\pi\\
&\cdot p_K p_\pi\cdot p_\pi B_0(q,m_K,m_\pi) + \frac{25}{3}\alpha_1 k_\pi\cdot p_K p_\pi\cdot p_\pi B_0(q,m_\eta,m_K) + \frac{3}{2}\alpha_1 k_\pi\\
&\cdot p_\pi B_0(q,m_K,m_\pi) m_K^2 - \frac{2}{3}\alpha_1 p_\pi\cdot p_\pi B_1(q,m_K,m_\pi) + \frac{10}{3}\alpha_1 p_\pi\cdot p_\pi B_1(q,m_\eta,m_K)\\
&+ \frac{8}{3}\alpha_2 k_\pi\cdot p_\pi B_0(q,m_K,m_\pi) m_K^2 + \frac{1}{2}\alpha_1 k_\pi\cdot p_\pi B_0(q,m_\eta,m_K) m_K^2\\
&+ \frac{3}{2}\alpha_1 p_K\cdot p_\pi B_0(q,m_K,m_\pi) m_K^2 + \frac{8}{3}\alpha_2 p_K\cdot p_\pi B_0(q,m_K,m_\pi) m_K^2 + \frac{1}{2}\alpha_1 p_K\\
&\cdot p_\pi B_0(q,m_\eta,m_K) m_K^2 - \frac{5}{6}\alpha_1 p_\pi\cdot p_\pi B_0(q,m_K,m_\pi) m_K^2 - \frac{85}{18}\alpha_1 p_\pi\cdot p_\pi B_0(q,m_\eta,m_K) m_K^2\\
&+ \frac{3}{2}\alpha_1 k_\pi\cdot p_\pi B_0(q,m_K,m_\pi) m_\pi^2 - \frac{8}{3}\alpha_2 k_\pi\cdot p_\pi B_0(q,m_K,m_\pi) m_\pi^2 + \frac{1}{2}\alpha_1 k_\pi\\
&\cdot p_\pi B_0(q,m_\eta,m_K) m_\pi^2 + \frac{3}{2}\alpha_1 p_K\cdot p_\pi B_0(q,m_K,m_\pi) m_\pi^2 - \frac{8}{3}\alpha_2 p_K\cdot p_\pi B_0(q,m_K,m_\pi) m_\pi^2\\
&+ \frac{1}{2}\alpha_1 p_K\cdot p_\pi B_0(q,m_\eta,m_K) m_\pi^2 - \frac{5}{6}\alpha_1 p_\pi\cdot p_\pi B_0(q,m_K,m_\pi) m_\pi^2 - \frac{5}{18}\alpha_1 p_\pi\\
&\cdot p_\pi B_0(q,m_\eta,m_K) m_\pi^2 - 2\alpha_1 k_\pi\cdot p_\pi B_0(q,m_K,m_\pi)\cdot p_\pi - 10\alpha_1 k_\pi\cdot p_\pi B_0(q,m_\eta,m_K)\\
&\cdot p_\pi - 2\alpha_1 p_\pi\cdot p_\pi B_0(q,m_K,m_\pi)\cdot p_K + \frac{1}{24}\alpha_1(-m_K^2 - m_\pi^2 + 2k_\pi\cdot p_K - 2k_\pi\cdot p_\pi\\
&+ 2p_K\cdot p_\pi)(50k_\pi\cdot p_K - 23(m_K^2 + m_\pi^2)) B_0(q,m_K,m_\pi)\\
&+ \frac{2}{9}\alpha_2(m_K^2 - m_\pi^2)(7(m_K^2 + m_\pi^2) - 10k_\pi\cdot p_K) B_0(q,m_K,m_\pi)\\
&+ \frac{1}{72}\alpha_1(m_K^2 + m_\pi^2 - 2k_\pi\cdot p_K + 2k_\pi\cdot p_\pi - 2p_K\cdot p_\pi)(17m_K^2 + m_\pi^2 - 30k_\pi\cdot p_K)\\
&\times B_0(q,m_\eta,m_K) + \frac{1}{3}\alpha_1(-14m_K^2 - 14m_\pi^2 + 30k_\pi\cdot p_K - 5k_\pi\cdot p_\pi + 5p_K\cdot p_\pi)\\
&\times B_1(q,m_K,m_\pi) + \frac{1}{9}\alpha_1(-10m_K^2 - 2m_\pi^2 + 18k_\pi\cdot p_K - 3k_\pi\cdot p_\pi + 3p_K\cdot p_\pi)\\
&\times B_1(q,m_\eta,m_K) - \frac{8}{9}\alpha_2(m_K^2 - m_\pi^2) B_1(q,m_K,m_\pi) + \frac{10}{3}\alpha_1 B_2(q,m_K,m_\pi)\\
&+ \frac{2}{3}\alpha_1 B_2(q,m_\eta,m_K)\Big)
\end{aligned}$$

4. Diagram H2

Here, $q = -\frac{1}{2}(p_K + p_\pi)$,

$$\begin{aligned}\langle \pi^-(k_\pi)|\mathcal{O}^{(8,1)}|K^0(p_K)\pi^-(p_\pi)\rangle_{H2} = \frac{1}{f^5\pi^2}\Big(&\frac{4}{3}\alpha_1 k_\pi \cdot B_0(q, m_K, m_\pi)m_K^2 - \frac{16}{3}\alpha_1 k_\pi \cdot B_1(q, m_K, m_\pi) \\ &+ \frac{40}{3}\alpha_1 k_\pi \cdot B_0(q, m_K, m_\pi)p_K \cdot p_\pi + \frac{4}{3}\alpha_1 k_\pi \cdot B_0(q, m_K, m_\pi)m_\pi^2 \\ &- \frac{4}{9}\alpha_2(m_K^2 - m_\pi^2)(m_K^2 + m_\pi^2 + 10p_K \cdot p_\pi)B_0(q, m_K, m_\pi) \\ &+ \frac{16}{9}\alpha_2(m_K^2 - m_\pi^2)B_1(q, m_K, m_\pi)\Big)\end{aligned}$$

5. Diagram H3

$$\begin{aligned}\langle \pi^-(k_\pi)|\mathcal{O}^{(8,1)}|K^0(p_K)\pi^-(p_\pi)\rangle_{H3} = \frac{1}{f^5\pi^2}\Big(&\frac{64}{15}(-35\alpha_1 k_\pi \cdot p_K + 5\alpha_1 p_K \cdot p_\pi + 2(25\alpha_1 k_\pi \cdot p_\pi + 7\alpha_2(m_K^2 - m_\pi^2))) \\ &\times A_0(m_K) - \frac{32}{3}(-4\alpha_2 m_K^2 + 4\alpha_2 m_\pi^2 + 10\alpha_1 k_\pi \cdot p_K - 7\alpha_1 k_\pi \cdot p_\pi + 5\alpha_1 p_K \cdot p_\pi) \\ &\times A_0(m_\pi) + \frac{32}{45}(8\alpha_2 m_K^2 - 8\alpha_2 m_\pi^2 - 90\alpha_1 k_\pi \cdot p_K + 45\alpha_1 k_\pi \cdot p_\pi + 45\alpha_1 p_K \cdot p_\pi) \\ &\times A_0(m_\eta) - 64\alpha_1 A_1(m_K) + \frac{224}{3}\alpha_1 A_1(m_\pi) - \frac{32}{3}\alpha_1 A_1(m_\eta)\Big)\end{aligned}$$

6. Diagram D12a

Here, $q = \frac{1}{2}(p_K + p_\pi)$,

$$\begin{aligned}\langle \pi^-(k_\pi)|\mathcal{O}^{(8,1)}|K^0(p_K)\pi^-(p_\pi)\rangle_{D12a} = \frac{\alpha_2(m_K^2 - m_\pi^2)}{4f^5\pi^2}\frac{-1}{(p_k + p_\pi - k_\pi)^2 - m_K^2}\Big(&-\frac{1}{36}(m_K^2 - 3m_\pi^2 + 4k_\pi \cdot p_K + 4k_\pi \cdot p_\pi \\ &+ 6p_K \cdot p_\pi)(m_K^2 + m_\pi^2 + 10p_K \cdot p_\pi)B_0(q, m_K, m_\pi) \\ &+ \frac{2}{9}(m_K^2 - m_\pi^2 + 2k_\pi \cdot p_K + 2k_\pi \cdot p_\pi + 8p_K \cdot p_\pi)B_1(q, m_K, m_\pi) \\ &- \frac{4}{9}B_2(q, m_K, m_\pi)\Big)\end{aligned}$$

7. Diagram D12b

Here, $q = \frac{1}{2}(k_\pi - p_\pi)$,

$$\begin{aligned}\langle \pi^-(k_\pi)|\mathcal{O}^{(8,1)}|K^0(p_K)\pi^-(p_\pi)\rangle_{D12b} = {} & \frac{\alpha_2(m_K^2 - m_\pi^2)}{4f^5\pi^2}\,\frac{-1}{(p_k + p_\pi - k_\pi)^2 - m_K^2} \\ & \times \Big(-\frac{5}{3}p_K \cdot B_1(q, m_K, m_\pi) - p_K \cdot B_1(q, m_\eta, m_K) - \frac{5}{3}p_\pi \cdot B_1(q, m_K, m_\pi) \\ & - p_\pi \cdot B_1(q, m_\eta, m_K) - \frac{1}{12}p_K \cdot B_0(q, m_K, m_\pi)(-23m_K^2 - 13m_\pi^2 + 40k_\pi \cdot p_K \\ & - 10k_\pi \cdot p_\pi + 10p_K \cdot p_\pi) + \frac{5}{6}k_\pi \cdot B_0(q, m_K, m_\pi)(-m_\pi^2 + k_\pi \cdot p_K + k_\pi \cdot p_\pi \\ & - p_K \cdot p_\pi) + \frac{1}{2}k_\pi \cdot B_0(q, m_\eta, m_K)(-m_\pi^2 + k_\pi \cdot p_K + k_\pi \cdot p_\pi - p_K \cdot p_\pi) \\ & - \frac{1}{12}p_\pi \cdot B_0(q, m_\eta, m_K)(-17m_K^2 - m_\pi^2 + 30k_\pi \cdot p_K) - \frac{1}{12}p_K \\ & \cdot B_0(q, m_\eta, m_K)(-17m_K^2 + 5m_\pi^2 + 24k_\pi \cdot p_K - 6k_\pi \cdot p_\pi + 6p_K \cdot p_\pi) \\ & - \frac{1}{12}p_\pi \cdot B_0(q, m_K, m_\pi)(50k_\pi \cdot p_K - 23(m_K^2 + m_\pi^2)) + \frac{3}{2}k_\pi \cdot B_0(q, m_K, m_\pi) \cdot k_\pi \\ & - 3k_\pi \cdot B_0(q, m_K, m_\pi) \cdot p_\pi + \frac{3}{2}k_\pi \cdot B_0(q, m_\eta, m_K) \cdot k_\pi - 3k_\pi \cdot B_0(q, m_\eta, m_K) \\ & \cdot p_\pi - \frac{3}{2}p_K \cdot B_0(q, m_K, m_\pi) \cdot p_K - \frac{3}{2}p_K \cdot B_0(q, m_\eta, m_K) \cdot p_K - 3p_\pi \\ & \cdot B_0(q, m_K, m_\pi) \cdot p_K - 3p_\pi \cdot B_0(q, m_\eta, m_K) \cdot p_K - \frac{1}{32}(-3m_K^2 + m_\pi^2 + 6k_\pi \cdot p_K \\ & - 4k_\pi \cdot p_\pi + 4p_K \cdot p_\pi)(10k_\pi \cdot p_K - 3(m_K^2 + m_\pi^2))B_0(q, m_K, m_\pi) \\ & - \frac{1}{144}(7m_K^2 + 3m_\pi^2 - 6k_\pi \cdot p_K + 4k_\pi \cdot p_\pi - 4p_K \cdot p_\pi)(7(m_K^2 + m_\pi^2) \\ & - 10k_\pi \cdot p_K)B_0(q, m_K, m_\pi) - \frac{1}{144}(7m_K^2 + 3m_\pi^2 - 6k_\pi \cdot p_K + 4k_\pi \cdot p_\pi \\ & - 4p_K \cdot p_\pi)(7(m_K^2 + m_\pi^2) - 10k_\pi \cdot p_K)B_0(q, m_K, m_\pi) \\ & - \frac{1}{864}(17m_K^2 - 11m_\pi^2 - 18k_\pi \cdot p_K + 12k_\pi \cdot p_\pi - 12p_K \cdot p_\pi)(17m_K^2 + m_\pi^2 \\ & - 30k_\pi \cdot p_K)B_0(q, m_\eta, m_K) + \frac{1}{4}(3m_K^2 + m_\pi^2 - 8k_\pi \cdot p_K + 2k_\pi \cdot p_\pi - 2p_K \cdot p_\pi) \\ & \times B_1(q, m_K, m_\pi) + \frac{1}{18}(7m_K^2 + 5m_\pi^2 - 8k_\pi \cdot p_K + 2k_\pi \cdot p_\pi - 2p_K \cdot p_\pi) \\ & \times B_1(q, m_K, m_\pi) - \frac{11}{18}B_2(q, m_K, m_\pi) - \frac{1}{6}B_2(q, m_\eta, m_K)\Big)\end{aligned}$$

8. Diagram D12c

Here, $q = \frac{1}{2}(p_K - k_\pi)$,

$$\begin{aligned}\langle \pi^-(k_\pi)|\mathcal{O}^{(8,1)}|K^0(p_K)\pi^-(p_\pi)\rangle_{D12c} = {} & \frac{\alpha_2(m_K^2 - m_\pi^2)}{4f^5\pi^2}\frac{-1}{(p_k + p_\pi - k_\pi)^2 - m_K^2} \\ & \times \Big(k_\pi \cdot B_0(q, m_K, m_K)\cdot k_\pi - 2k_\pi \cdot B_0(q, m_K, m_K)\cdot p_K + 2k_\pi \cdot B_0(q, m_\pi, m_\pi) \\ & \cdot k_\pi - 4k_\pi \cdot B_0(q, m_\pi, m_\pi)\cdot p_K - 2p_\pi \cdot B_0(q, m_K, m_K)\cdot p_K - p_\pi \\ & \cdot B_0(q, m_K, m_K)\cdot p_\pi - 4p_\pi \cdot B_0(q, m_\pi, m_\pi)\cdot p_K - 2p_\pi \cdot B_0(q, m_\pi, m_\pi)\cdot p_\pi \\ & + \frac{1}{12}(-2m_K^2 - 5m_\pi^2 + 5k_\pi \cdot p_\pi)(2m_K^2 + 3m_\pi^2 + 2k_\pi \cdot p_K - 3k_\pi \cdot p_\pi \\ & - 2p_K \cdot p_\pi)B_0(q, m_K, m_K) + \frac{1}{18}(5k_\pi \cdot p_\pi - 7m_\pi^2)(5m_\pi^2 + 2k_\pi \cdot p_K - 3k_\pi \cdot p_\pi \\ & - 2p_K \cdot p_\pi)B_0(q, m_\pi, m_\pi) + \frac{1}{18}(5k_\pi \cdot p_\pi - 4m_\pi^2)(5m_\pi^2 + 2k_\pi \cdot p_K - 3k_\pi \cdot p_\pi \\ & - 2p_K \cdot p_\pi)B_0(q, m_\pi, m_\pi) - \frac{1}{18}m_\pi^2(7m_\pi^2 + 6k_\pi \cdot p_K - 9k_\pi \cdot p_\pi - 6p_K \cdot p_\pi) \\ & \times B_0(q, m_\eta, m_\eta) + \frac{1}{3}(2m_K^2 + 4m_\pi^2 + k_\pi \cdot p_K - 4k_\pi \cdot p_\pi - p_K \cdot p_\pi) \\ & \times B_1(q, m_K, m_K) + \frac{2}{9}(6m_\pi^2 + k_\pi \cdot p_K - 4k_\pi \cdot p_\pi - p_K \cdot p_\pi)B_1(q, m_\pi, m_\pi) \\ & + \frac{1}{9}(9m_\pi^2 + 2k_\pi \cdot p_K - 8k_\pi \cdot p_\pi - 2p_K \cdot p_\pi)B_1(q, m_\pi, m_\pi) \\ & + \frac{1}{3}B_1(q, m_\eta, m_\eta)m_\pi^2 - \frac{1}{3}B_2(q, m_K, m_K) - \frac{4}{9}B_2(q, m_\pi, m_\pi)\Big)\end{aligned}$$

9. Diagram D3

$$\begin{aligned}\langle \pi^-(k_\pi)|\mathcal{O}^{(8,1)}|K^0(p_K)\pi^-(p_\pi)\rangle_{D3} = {} & \frac{\alpha_2(m_K^2 - m_\pi^2)}{4f^5\pi^2}\frac{-1}{(p_k + p_\pi - k_\pi)^2 - m_K^2} \\ & \times \Big(\frac{32}{45}(-18k_\pi \cdot k_\pi + 13k_\pi \cdot p_K + 18k_\pi \cdot p_\pi + 17p_K \cdot p_K + 47p_K \cdot p_\pi \\ & + 12p_\pi \cdot p_\pi)A_0(m_K) + \frac{16}{9}(-8k_\pi \cdot k_\pi + 13k_\pi \cdot p_K + 8k_\pi \cdot p_\pi + 2p_K \cdot p_K \\ & + 17p_K \cdot p_\pi + 7p_\pi \cdot p_\pi)A_0(m_\pi) + \frac{16}{15}(-4k_\pi \cdot k_\pi - k_\pi \cdot p_K + 4k_\pi \cdot p_\pi \\ & + 6p_K \cdot p_K + 11p_K \cdot p_\pi + p_\pi \cdot p_\pi)A_0(m_\eta) + \frac{544}{45}A_1(m_K) + \frac{112}{9}A_1(m_\pi) \\ & + \frac{16}{15}A_1(m_\eta)\Big)\end{aligned}$$

10. Diagram F1

$$\begin{aligned}\langle \pi^+(k_\pi)|\mathcal{O}^{(8,1)}|K^+(p_K)\rangle\rangle_{F3} = {} & \frac{i}{f^4\pi^2}\Big(-\frac{64}{3}(7\alpha_1 k_\pi \cdot p_K - 4\alpha_2 m_K^2)A_0(m_K) - \frac{160}{3}(2\alpha_1 k_\pi \cdot p_K - \alpha_2 m_K^2)A_0(m_\pi) \\ & - \frac{32}{3}(6\alpha_1 k_\pi \cdot p_K - \alpha_2 m_K^2)A_0(m_\eta) - 64\alpha_1 A_1(m_K) + \frac{64}{3}\alpha_1 A_1(m_\pi)\Big)\end{aligned}$$

11. Diagram F2

Here, $q = \frac{1}{2}(k_\pi - p_\pi)$,

$$\begin{aligned}\langle \pi^+(k_\pi)|\mathcal{O}^{(8,1)}|K^+(p_K)\rangle_{F2} = \frac{i}{f^4\pi^2}\Big(&6\alpha_1 k_\pi\cdot B_1(q,m_K,m_\pi) - 2\alpha_1 k_\pi\cdot B_1(q,m_K,m_\eta) + 6\alpha_1 p_K\cdot B_1(q,m_K,m_\pi)\\ &-\frac{3}{2}\alpha_1 k_\pi\cdot B_0(q,m_K,m_\pi)m_\pi^2 + \frac{1}{2}\alpha_1 k_\pi\cdot B_0(q,m_K,m_\eta)m_\pi^2 - 2\alpha_1 p_K\cdot B_1(q,m_K,m_\eta)\\ &+\frac{1}{2}\alpha_1 p_K\cdot B_0(q,m_K,m_\eta)m_\pi^2 - \frac{3}{2}\alpha_1 p_K\cdot B_0(q,m_K,m_\pi)m_\pi^2 + \frac{1}{24}\alpha_1 m_\pi^2(8m_K^2+13m_\pi^2\\ &-20k_\pi\cdot p_K + 10k_\pi\cdot p_\pi - 10p_K\cdot p_\pi)B_0(q,m_K,m_\pi) - \frac{1}{72}\alpha_1 m_\pi^2(-8m_K^2+5m_\pi^2+12k_\pi\\ &\cdot p_K - 6k_\pi\cdot p_\pi + 6p_K\cdot p_\pi)B_0(q,m_K,m_\eta) + \frac{1}{3}\alpha_1(-4m_K^2-9m_\pi^2+10k_\pi\cdot p_K - 5k_\pi\\ &\cdot p_\pi + 5p_K\cdot p_\pi)B_1(q,m_K,m_\pi) + \frac{1}{9}\alpha_1(-4m_K^2+m_\pi^2+6k_\pi\cdot p_K - 3k_\pi\cdot p_\pi + 3p_K\\ &\cdot p_\pi)B_1(q,m_K,m_\eta) + \frac{10}{3}\alpha_1 B_2(q,m_K,m_\pi) + \frac{2}{3}\alpha_1 B_2(q,m_K,m_\eta)\Big)\end{aligned}$$

12. Diagram A3

$$\begin{aligned}\langle \pi^-(k_\pi)|\mathcal{O}^{(8,1)}|K^0(p_K)\pi^-(p_\pi)\rangle_{A3} = \frac{1}{f^5\pi^2}\Big(&-\frac{128\alpha_2(-2m_\pi^2+2k_\pi\cdot p_K+2k_\pi\cdot p_\pi+4p_K\cdot p_\pi)(m_K^2-m_\pi^2)A_0(m_K)}{3(2m_\pi^2-2k_\pi\cdot p_K-2k_\pi\cdot p_\pi+2p_K\cdot p_\pi)}\\ &-\frac{128\alpha_2(-2m_\pi^2+2k_\pi\cdot p_K+2k_\pi\cdot p_\pi+4p_K\cdot p_\pi)(m_K^2-m_\pi^2)A_0(m_K)}{3(2m_\pi^2-2k_\pi\cdot p_K-2k_\pi\cdot p_\pi+2p_K\cdot p_\pi)}\\ &-\frac{64\alpha_2(-2m_\pi^2+2k_\pi\cdot p_K+2k_\pi\cdot p_\pi+4p_K\cdot p_\pi)(m_K^2-m_\pi^2)A_0(m_\pi)}{3(2m_\pi^2-2k_\pi\cdot p_K-2k_\pi\cdot p_\pi+2p_K\cdot p_\pi)}\\ &-\frac{64\alpha_2(-2m_\pi^2+2k_\pi\cdot p_K+2k_\pi\cdot p_\pi+4p_K\cdot p_\pi)(m_K^2-m_\pi^2)A_0(m_\eta)}{9(2m_\pi^2-2k_\pi\cdot p_K-2k_\pi\cdot p_\pi+2p_K\cdot p_\pi)}\\ &+\frac{64\alpha_1(-2m_\pi^2+2k_\pi\cdot p_K+2k_\pi\cdot p_\pi+4p_K\cdot p_\pi)A_1(m_K)}{3(2m_\pi^2-2k_\pi\cdot p_K-2k_\pi\cdot p_\pi+2p_K\cdot p_\pi)}\\ &-\frac{32\alpha_1(-2m_\pi^2+2k_\pi\cdot p_K+2k_\pi\cdot p_\pi+4p_K\cdot p_\pi)A_1(m_\pi)}{2m_\pi^2-2k_\pi\cdot p_K-2k_\pi\cdot p_\pi+2p_K\cdot p_\pi}\\ &+\frac{32\alpha_1(-2m_\pi^2+2k_\pi\cdot p_K+2k_\pi\cdot p_\pi+4p_K\cdot p_\pi)A_1(m_\eta)}{3(2m_\pi^2-2k_\pi\cdot p_K-2k_\pi\cdot p_\pi+2p_K\cdot p_\pi)}\Big)\end{aligned}$$

APPENDIX B: FINITE VOLUME EFFECTS

The following argument follows Ref. [36], where more detailed discussion can be found. The relevant correlation function is

$$\begin{aligned}\mathcal{C}(t) &\equiv \int_V d^x e^{\mathbf{P}\cdot\mathbf{x}}\langle\pi(\mathbf{k}_\pi)|H_W(0)\mathcal{O}_{K\pi}(t,x)|0\rangle\\ &\approx V\sum_n\langle\pi(\mathbf{k}_\pi)|H_W(0)|K\pi,n,\mathbf{P}\rangle\\ &\quad\times e^{-E_n t}\langle K\pi,n,\mathbf{P}|\mathcal{O}_{K\pi}(0)|0\rangle,\end{aligned}\tag{B1}$$

where contributions from excited state e.g. four particle states are ignored since we are interested in the asymptotic limit in which $t\to\infty$.

If the volume is sufficiently large, the summation can be approximated with integration:

$$\begin{aligned}\mathcal{C}(t) = V\int_0^\infty dE\rho_V(E)e^{-Et}&\langle\pi(\mathbf{k}_\pi)|H_W(0)|K\pi,(E,\mathbf{P})\rangle\\ &\times\langle K\pi,(E,\mathbf{P})|\mathcal{O}_{K\pi}(0)|0\rangle,\end{aligned}\tag{B2}$$

where the interpretation of $\rho_V(E)$ is given in Ref. [36]. Roughly, ρ_V can be understood as density of states.

Meanwhile, the large volume allows us to rewrite the correlation function, $\mathcal{C}(t)$, in terms of infinite volume

asymptotic states:

$$\mathcal{C}(t) = \left(\frac{1}{2\pi}\right)^6 \int \frac{dp_1^3}{2E_1}\frac{dp_2^3}{2E_2}\langle\pi(\mathbf{k}_\pi)|H_W(0)|K(\mathbf{p}_1)\pi(\mathbf{p}_2)\rangle\langle K(\mathbf{p}_1)\pi(\mathbf{p}_2)|\mathcal{O}_{K\pi}|0\rangle. \tag{B3}$$

We perform a small manipulation on the above equation using

$$\begin{aligned}\langle K(\mathbf{p}_K)\pi(\mathbf{p}_\pi)|\mathcal{O}_{K\pi}(t,\mathbf{P})|0\rangle &= \int d^3x e^{i\mathbf{P}\cdot\mathbf{x}}\langle K(\mathbf{p}_K)\pi(\mathbf{p}_\pi)|\mathcal{O}_{K\pi}(t,\mathbf{x})|0\rangle \\ &= \int d^3x e^{i\mathbf{P}\cdot\mathbf{x}}e^{-i(\mathbf{p}_K+\mathbf{p}_\pi)\cdot\mathbf{x}}e^{-Et}\langle K(\mathbf{p}_K)\pi(\mathbf{p}_\pi)|\mathcal{O}_{K\pi}(0)|0\rangle \\ &= (2\pi)^3\delta(\mathbf{P}-\mathbf{p}_K-\mathbf{p}_\pi)\langle K(\mathbf{p}_K)\pi(\mathbf{p}_\pi)|\mathcal{O}_{K\pi}(0)|0\rangle e^{-Et},\end{aligned}$$

where

$$E = E_K(\mathbf{p}_K) + E_\pi(\mathbf{p}_\pi), \qquad E_i(\mathbf{p}) = \sqrt{m_i^2+\mathbf{p}^2}. \tag{B4}$$

Then the correlation function can be written in terms of the four-momentum integral:

$$\begin{aligned}\langle\pi(\mathbf{k}_\pi)|H_W(0)\mathcal{O}_{K\pi}(t,\mathbf{P})|0\rangle = (2\pi)^3\int dE\int\frac{dp_K^4}{(2\pi)^4}\frac{dp_\pi^4}{(2\pi)^4}\delta^+(p_K^2-m_K^2)\delta^+(p_\pi^2-m_\pi^2)\delta^4(P-p_K-p_\pi) \\ \times e^{-(E_K+E_\pi)t}\langle\pi(\mathbf{k}_\pi)|H_W(0)|K(p_K)\pi(p_\pi)\rangle\langle K(p_K)\pi(p_\pi)|\mathcal{O}_{K\pi}(0)|0\rangle,\end{aligned}$$

where

$$p_i = (E_i, \mathbf{p}_i). \tag{B5}$$

Since the integral is in covariant form, one can easily change the integration variables with Lorentz-transformed ones which brings the two particle state into CM frame:

$$\begin{aligned}\langle\pi(\mathbf{k}_\pi)|H_W(0)\mathcal{O}_{K\pi}(t,\mathbf{P})|0\rangle = (2\pi)^3\int dE\int\frac{dq_K^4}{(2\pi)^4}\frac{dq_\pi^4}{(2\pi)^4}\delta^+(q_K^2-m_K^2)\delta^+(q_\pi^2-m_\pi^2)\delta(E^*-E_K^*-E_\pi^*)\delta^3(\mathbf{q}_K+\mathbf{q}_\pi) \\ \times e^{-Et}\langle\pi(\mathbf{k}_\pi^*)|H_W(0)|K(q_K)\pi(q_\pi)\rangle\langle K(q_K)\pi(q_\pi)|\mathcal{O}_{K\pi}(0)|0\rangle.\end{aligned} \tag{B6}$$

Note that the amplitudes are treated as scalars. Using the δ function, one can do some integrations,

$$\begin{aligned}\langle\pi(\mathbf{k}_\pi)|H_W(0)\mathcal{O}_{K\pi}(t,\mathbf{P})|0\rangle = (2\pi)^{-3}\int dE e^{-Et}\int\frac{dq^3}{2E_K(\mathbf{q})2E_\pi(\mathbf{q})}\delta(E^*-E_K(\mathbf{q})-E_\pi(\mathbf{q}))\langle\pi(\mathbf{k}_\pi^*)|H_W(0)|K(\mathbf{q})\pi(-\mathbf{q})\rangle \\ \times\langle K(\mathbf{q})\pi(-\mathbf{q})|\mathcal{O}_{K\pi}(0)|0\rangle,\end{aligned}$$

where E_K^* and E_π^* of Eq. (B6) are fixed, respectively, by

$$E_K(\mathbf{q}) = \sqrt{m_K^2+\mathbf{q}^2}, \qquad E_\pi(\mathbf{q}) = \sqrt{m_\pi^2+\mathbf{q}^2}. \tag{B7}$$

In order to proceed, we have to assume that the creation operator $\mathcal{O}_{K\pi}$ is chosen so that $\langle K(\mathbf{q})\pi(-\mathbf{q})|\mathcal{O}_{K\pi}(0)|0\rangle$ does not have angular dependence. In fact, the contribution originating from the particular form of $O_{K\pi}$ will be canceled in the end. The role of $O_{K\pi}$ is restricted to keeping the initial states in S-wave. With this assumption, a further simplification is possible:

$$\begin{aligned}&\langle\pi(\mathbf{k}_\pi)|H_W(0)\mathcal{O}_{K\pi}(t,\mathbf{P})|0\rangle \\ &= (2\pi)^{-3}\int dE e^{-Et}\frac{1}{q^*}\frac{E_K(q^*)E_\pi(q^*)}{E_K(q^*)+E_\pi(q^*)} \\ &\times\langle K(\mathbf{q}^*)\pi(-\mathbf{q}^*)|\mathcal{O}_{K\pi}(0)|0\rangle \\ &\times\int d\Omega\langle\pi(\mathbf{k}_\pi^*)|H_W(0)|K(\mathbf{q})\pi(-\mathbf{q})\rangle,\end{aligned} \tag{B8}$$

where q^* is defined as

$$E^* = \sqrt{m_K^2+q^{*2}}+\sqrt{m_\pi^2+q^{*2}}. \tag{B9}$$

Since $\langle K(\mathbf{q}^*)\pi(-\mathbf{q}^*)|\mathcal{O}_{K\pi}(0)|0\rangle$ does not have any angular dependence, we write this as $\langle K\pi, E^*|\mathcal{O}_{K\pi}(0)|0\rangle$. Moreover, $\int d\Omega\langle\pi(\mathbf{k}_\pi^*)|H_W(0)|K(\mathbf{q})\pi(-\mathbf{q})\rangle$ is also a function of E^* because of angular averaging so we use a notation $d\Omega_{E^*}$.

By comparing Eqs. (B2) and (B8), one can deduce

$$\rho_V(E)\langle\pi(\mathbf{k}_\pi)|H_W(0)|K\pi,(E,\mathbf{P})\rangle\langle K\pi,(E,\mathbf{P})|\mathcal{O}_{K\pi}|0\rangle = \frac{1}{4(2\pi)^3}\left(\frac{q}{E^*}\right)\langle K\pi, E^*|\mathcal{O}_{K\pi}(0)|0\rangle \times \int d\Omega_{E^*}\langle\pi(k_\pi^*)|H_W(0)|K(\mathbf{q})\pi(-\mathbf{q})\rangle. \quad \text{(B10)}$$

However, Eq. (B10) is not satisfactory because of the appearance of an unknown factor $\langle K\pi, E^*|\mathcal{O}_{K\pi}(0)|0\rangle$. In order to eliminate this factor, we consider a correlation function,

$$\langle\mathcal{O}_{K\pi}(t,\mathbf{P})\mathcal{O}_{K\pi}^\dagger(0,\mathbf{P})\rangle. \quad \text{(B11)}$$

One can easily imagine that by similar argument, the following equation can be obtained:

$$\rho_V(E)|\langle K\pi,(E,\mathbf{P})|\mathcal{O}_{K\pi}|0\rangle|^2 = \frac{\pi}{(2\pi)^3}\left(\frac{q^*}{E^*}\right)|\langle K\pi, E^*|\mathcal{O}_{K\pi}(0)|0\rangle|^2. \quad \text{(B12)}$$

By dividing Eq. (B10) by the square root of Eq. (B12), the relation between matrix elements can be deduced,

$$|\langle\pi(\mathbf{k}_\pi)|H_W(0)|K\pi,(E,\mathbf{P})\rangle| = \frac{1}{4\pi}\frac{1}{\sqrt{\rho_V}}\sqrt{\frac{\pi}{(2\pi)^3}\left(\frac{q^*}{E^*}\right)} \times \left|\int d\Omega_{E^*}\langle\pi(\mathbf{k}_\pi^*)|H_W(0)|K(\mathbf{q})\pi(-\mathbf{q})\rangle\right|.$$

APPENDIX C: LECS FOR $\mathcal{O}^{\Delta I=1/2}_{(27,1)}$ AND $\mathcal{O}^{\Delta I=1/2}_{(8,8)}$

It has been argued that LECs for operators with (8, 8) $\Delta I = 1/2$ can determined without $K \to \pi\pi_{I=0}$ in Ref. [7]. In this section, we will show that LECs for operators with (27, 1) $\Delta I = 1/2$ as well can be determined without calculating $\Delta I = 1/2$, $K \to \pi\pi_{I=0}$ matrix elements. Its analytic term at physical kinematics is given by

$$-\frac{4i(m_K^2-m_\pi^2)}{f^3}[-\alpha_{27}+(d_4+d_5-9d_6+4d_7)m_K^2 + 2(-6d_1-2d_2+2d_4+6d_6+d_7-2d_{20}+8d_{24})m_\pi^2]. \quad \text{(C1)}$$

The $K \to \pi$ transition amplitudes with (27, 1) $\Delta I = 3/2$, are

$$\frac{1}{f^2}[-4\alpha_{27}(p_K\cdot k_\pi)+64d_{24}(p_K\cdot k_\pi)^2 + 8(d_4+d_7-d_{20})m_\pi^2(p_K\cdot k_\pi) + m_K^2(8(d_4+2d_7-d_{20})(p_K\cdot k_\pi)-16d_2m_\pi^2)]. \quad \text{(C2)}$$

From the above, one can determine α_{27}, d_2, d_7, $d_{20}-d_4$, d_{24} by varying masses and momenta.

The χPT formula for the $K \to \pi\pi_{I=2}$ transition amplitude with unphysical kinematics corresponding to the initial kaon and the final pions are at rest, is given by

$$-\frac{8im_\pi}{f^3}[-\alpha_{27}(m_K+m_\pi)/2+(d_4+d_5+4d_7-d_{20})m_K^3 + 2(d_{20}-d_2)m_\pi m_K^2+(3d_4+d_5+2d_7-3d_{20})m_\pi^2 m_K + 2d_2m_\pi^3]. \quad \text{(C3)}$$

By inspecting the above formula, we can see that d_5-d_4 can be determined. Since the χPT formula for the $K \to$ vac transition amplitude is

$$\frac{48id_1(m_K^2-m_\pi^2)^2}{f}, \quad \text{(C4)}$$

d_1 can be fixed from this. Finally, d_6 can be determined by using the $\Delta I = 1/2$ $K \to \pi$ transition amplitude whose χPT formula is

$$\frac{1}{f^2}[-4\alpha_{27}(p_K\cdot k_\pi)+(8(d_4-3d_6+2d_7-d_{20})(p_K\cdot k_\pi) - 16(3d_1+d_2)m_\pi^2)m_K^2+48d_1m_K^4+64d_{24}(p_K\cdot k_\pi)^2 + 8(d_4+3d_6+d_7-d_{20})(p_K\cdot k_\pi)m_\pi^2]. \quad \text{(C5)}$$

Since α_{27}, d_1, d_2, d_5-d_4, d_6, d_7, $d_{20}-d_4$, d_{24} are determined, one can reconstruct the physical $K \to \pi\pi$ transition amplitude with (27, 1) $\Delta I = 1/2$ using Eq. (C1).

APPENDIX D: PROOF

We prove the case where the new measurement is uncorrelated to the other matrix elements and then give comments on the general case.

With the assumption that a new measurement is uncorrelated, we write the new correlation matrix as

$$\bar{\Sigma} = \begin{pmatrix}\Sigma & \\ & \sigma\end{pmatrix}, \qquad \bar{\Sigma}^{-1} = \begin{pmatrix}\Sigma^{-1} & \\ & \sigma^{-1}\end{pmatrix}. \quad \text{(D1)}$$

By writing the new kinematic matrix as

$$\bar{K} = \begin{pmatrix}K\\ N\end{pmatrix}, \quad \text{(D2)}$$

the correlation of LECs can be written

$$\langle X_iX_j\rangle = [(\bar{K}^T\bar{\Sigma}^{-1}\bar{K})^{-1}]_{ij} = [(K^T\Sigma^{-1}K+N^T\sigma^{-1}N)^{-1}]_{ij}. \quad \text{(D3)}$$

With defining

$$C = K^T \Sigma^{-1} K, \qquad \bar{C} = C + N^T \sigma^{-1} N, \tag{D4}$$

we want to prove that the diagonal elements of C^{-1} are larger than those of $\bar{C}^{-1}$.

If we write $d \equiv \bar{C}^{-1} - C^{-1}$, we have

$$(C + f^T f) \cdot (C^{-1} + d) = I, \tag{D5}$$

where $f \equiv N/\sqrt{\sigma}$. Expanding the above equation, we get

$$f^T f C^{-1} + Cd + f^T f d = 0. \tag{D6}$$

Multiplying C^{-1} from the left, we obtain

$$d = -C^{-1} f^T f (C^{-1} + d). \tag{D7}$$

We can solve for fd with multiplying f from the left:

$$fd = -fC^{-1}\left(\frac{fC^{-1}f^T}{fC^{-1}f^T + 1}\right). \tag{D8}$$

Then,

$$d = -C^{-1} f^T f C^{-1}\left(\frac{1}{fC^{-1}f^T + 1}\right). \tag{D9}$$

Since the matrix C^{-1} is positive definite and symmetric, $fC^{-1}f^T$ and the diagonal elements of $C^{-1}f^T f C^{-1}$ are positive. Therefore, the diagonal elements of d are negative.

As for the general case where the new measurement is correlated, one may be able to remove those correlations by a similarity transformation under which the covariance of the LECs is invariant (Eq. (31)).

This proves that increasing the number of kinematic points reduces the errors of the LECs.

[1] C. W. Bernard, T. Draper, G. Hockney, A. M. Rushton, and A. Soni, Phys. Rev. Lett. **55**, 2770 (1985).
[2] There are other methods that do not rely on chiral perturbation theory. See e.g. Refs. [3,4].
[3] M. Buchler, G. Colangelo, J. Kambor, and F. Orellana, Phys. Lett. B **521**, 22 (2001).
[4] C.-h. Kim and N. H. Christ, Nucl. Phys. B, Proc. Suppl. **119**, 365 (2003).
[5] T. Blum *et al.* (RBC Collaboration), Phys. Rev. D **68**, 114506 (2003).
[6] J. I. Noaki *et al.* (CP-PACS Collaboration), Phys. Rev. D **68**, 014501 (2003).
[7] J. Laiho and A. Soni, Phys. Rev. D **65**, 114020 (2002).
[8] C. Kim and C. T. Sachrajda, Proc. Sci., LAT2007 (2007) 357 [arXiv:0710.2519].
[9] A. Buras, M. Jamin, and M. E. Lautenbacher, Nucl. Phys. **B408**, 209 (1993).
[10] See, for example, [7,9].
[11] L. Lellouch and M. Luscher, Commun. Math. Phys. **219**, 31 (2001).
[12] In fact, α_2 does not appear in the physical transition amplitude. Hence, determining only α_1 is enough to obtain the physical amplitude, which can be easily done by choosing SU(3) limit.
[13] J. Kambor, J. Missimer, and D. Wyler, Nucl. Phys. **B346**, 17 (1990).
[14] J. Bijnens, E. Pallante, and J. Prades, Nucl. Phys. **B521**, 305 (1998).
[15] M. Golterman and E. Pallante, J. High Energy Phys. 08 (2000) 023.
[16] M. Golterman and E. Pallante, arXiv:hep-lat/0108029.
[17] V. Cirigliano and E. Golowich, Phys. Lett. B **475**, 351 (2000).
[18] C. J. D. Lin, G. Martinelli, E. Pallante, C. T. Sachrajda, and G. Villadoro, Nucl. Phys. **B650**, 301 (2003).
[19] For a detailed explanation, see Ref. [20] or Appendix C.
[20] C. J. D. Lin, G. Martinelli, C. T. Sachrajda, and M. Testa, Nucl. Phys. **B619**, 467 (2001).
[21] The product of the ordinary "CP" and "S" which is switching d and s-quark.
[22] C. Bernard, T. Draper, A. Soni, H. D. Politzer, and M. B. Wise, Phys. Rev. D **32**, 2343 (1985).
[23] J. Gasser and H. Leutwyler, Nucl. Phys. **B250**, 465 (1985).
[24] There are many ways to calculate those coefficients. For example, in Ref. [25], some of the coefficients are calculated with large errors. Although the Gasser-Leutwyler coefficients do not appear in the physical $K \to \pi\pi$ decay amplitude, their uncertainties result in poor determinations of some of the NLO LECs ($e_{35} - e_{15}$, e_{13}). Alternatively, one can consider a subtraction scheme introduced in Ref. [7] which cancels out the L_is. Since this subtraction may be necessary anyway in order to remove the mixing with lower dimensional operators, it may be useful to study the effect of the subtraction.
[25] C. Allton *et al.*, Phys. Rev. D **78**, 114509 (2008).
[26] If the SU(3) limit is taken, the tadpole contribution vanishes even though the denominator vanishes. The argument of Golterman *et al.* [27] can be applied for $K\pi \to \pi$ transitions, too.
[27] M. Golterman, C. J. D. Lin, and E. Pallante, Phys. Rev. D **69**, 057503 (2004).
[28] C. h. Kim, C. T. Sachrajda, and S. R. Sharpe, Nucl. Phys. **B727**, 218 (2005).
[29] N. H. Christ, C. Kim, and T. Yamazaki, Phys. Rev. D **72**, 114506 (2005).
[30] See Appendix B.
[31] S. Li and N. H. Christ, arXiv:0812.1368.
[32] Hence, the corresponding partially quenched chiral perturbation theory calculation of the matrix elements may be needed.

[33] C. Michael, Phys. Rev. D **49**, 2616 (1994).
[34] In such cases, one may consider adapting SU(2) χPT as in Ref. [25]. The immediate difficulty is that the external pions of the physical $K \to \pi\pi$ decay process have energy $m_K/2$. Hence, it is unclear how to treat these energetic pions in the approximation where m_K is taken to be large. Since there is an example to treat an energetic external pion [35] in SU(2) χPT, it may be possible to be generalized to the $K \to \pi\pi$ case, but it is not clear at the moment.
[35] J. M. Flynn and C. T. Sachrajda, Nucl. Phys. **B812**, 64 (2009).
[36] C. J. D. Lin, G. Martinelli, C. T. Sachrajda, and M. Testa, Nucl. Phys. B, Proc. Suppl. **109A**, 218 (2002).
[37] T. Hahn, Comput. Phys. Commun. **140**, 418 (2001).